Reports in Medical Imaging

Dovepress
open access to scientific and medical research

Open Access Full Text Article

REVIEW

Prostate cancer imaging: positron-emission tomography perspectives

This article was published in the following Dove Press journal:
Reports in Medical Imaging
15 April 2015
Number of times this article has been viewed

Nevein Ibrahim
Steve Y Cho

Department of Radiology, Nuclear Medicine Section, University of Wisconsin School of Medicine and Public Health, Madison, WI, USA

Abstract: There is a pressing demand for more accurate characterization of prostate cancer to provide risk-adapted patient-specific therapy, especially with the recent development of a growing repertoire of treatment options. This trend toward more personalized care has resulted in a need for improved prostate-specific imaging in order to provide image-guided therapy and facilitate treatment monitoring. In addition to these clinical needs, there is a growing vision and challenge for new molecular imaging techniques not only to detect tumors but also provide important information regarding tumor biology and prognosis. This review presents a perspective on prostate cancer imaging, summarizing current conventional imaging approaches with a focus on emerging and future positron emission tomography-based radiotracers at different clinical and preclinical stages of development.

Keywords: prostate cancer, positron-emission tomography, molecular imaging, single photon-emission computed tomography, prostate-specific membrane antigen

Introduction

Prostate cancer is among the most common male cancers, and is considered the second-leading cause of death among American men.[1] With the development of widening choices of therapeutic options and in order to provide image-guided therapy, facilitate therapeutic monitoring, and predict clinical outcome, more accurate characterization of prostate cancer is needed. Current NCCN Clinical Practice Guidelines In Oncology (NCCN Guidelines®) incorporate conventional imaging in the initial staging evaluation, as shown in Figure 1 (version 1.2015, http://www.nccn.org). The goal of prostate cancer imaging in the future will be to move beyond clinical management on the basis of current clinical risk factors (stage, serum prostate-specific antigen [PSA] level, and pathologic Gleason score)[2] to more individualized patient-adapted therapy based on prognostic biomarkers.[3,4] The trend toward more personalized care has resulted in a demand for more specialized imaging biomarkers and imaging techniques. Beyond the need for improved detection of the disease, there is a challenge for molecular imaging to assess its biology (indolent versus aggressive) and treatment response (castration-sensitive from castration-resistant prostate cancer [CRPC]).

This review summarizes imaging approaches in prostate cancer, focusing on current, emerging, and future positron-emission tomography (PET)-based molecular imaging agents in development, with a summary of the agents discussed provided in Table 1 and particular emphasis on their potential for mechanism-based and personalized approaches to disease management.

Correspondence: Steve Y Cho
Wisconsin Institutes for Medical Research – WIMR 7139, University of Wisconsin School of Medicine and Public Health, 1111 Highland Avenue, Madison, WI 53705, USA
Tel +1 608 263 5048
Fax +1 608 265 7390
Email scho@uwhealth.org

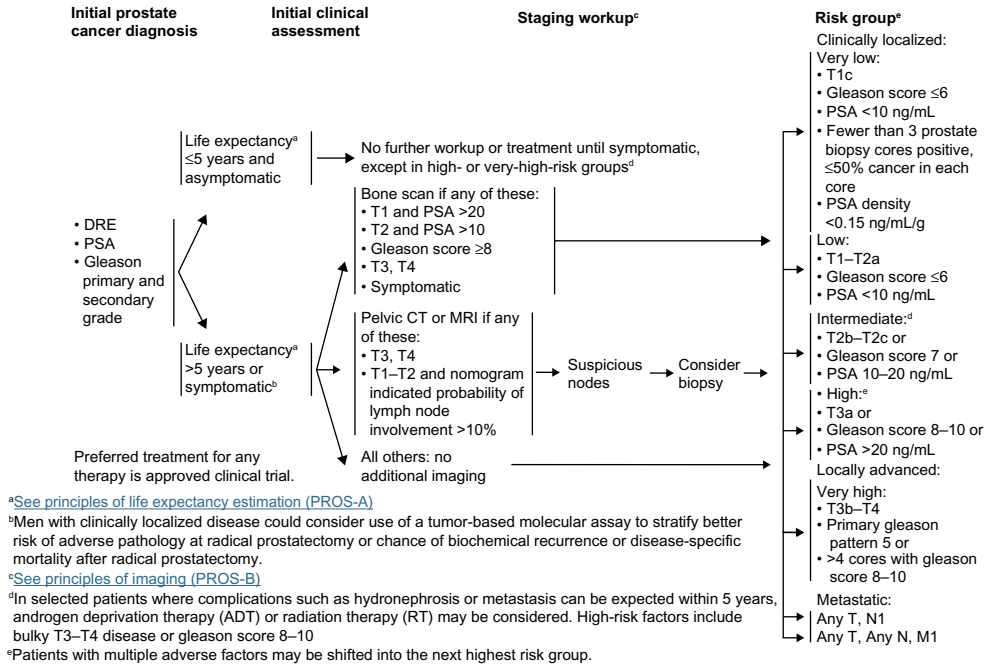

[a]See principles of life expectancy estimation (PROS-A)
[b]Men with clinically localized disease could consider use of a tumor-based molecular assay to stratify better risk of adverse pathology at radical prostatectomy or chance of biochemical recurrence or disease-specific mortality after radical prostatectomy.
[c]See principles of imaging (PROS-B)
[d]In selected patients where complications such as hydronephrosis or metastasis can be expected within 5 years, androgen deprivation therapy (ADT) or radiation therapy (RT) may be considered. High-risk factors include bulky T3–T4 disease or gleason score 8–10
[e]Patients with multiple adverse factors may be shifted into the next highest risk group.

Figure 1 NCCN guidelines in initial staging of prostate cancer.
Note: Adapted with permission from the NCCN Clinical Practice Guidelines in Oncology (NCCN Guidelines®) for Prostate Cancer V.1.2015. © 2014 National Comprehensive Cancer Network, Inc. All rights reserved. The NCCN Guidelines® and illustrations herein may not be reproduced in any form for any purpose without the express written permission of the NCCN. To view the most recent and complete version of the NCCN Guidelines, go online to NCCN.org. National Comprehensive Cancer Network®, NCCN®, NCCN Guidelines®, and all other NCCN Content are trademarks owned by the National Comprehensive Cancer Network, Inc.
Abbreviations: DRE, digital rectal exam; PSA, prostate-specific antigen; CT, computed tomography; MRI, magnetic resonance imaging; NCCN, National Comprehensive Cancer Network.

Table 1 Current and future molecular imaging agents in prostate cancer

Agents	Half-life	Technique	Mechanism/target
Current PET agents			
^{99m}Tc-MDP	6 hours	Planar/SPECT	Bisphosphonate analog
^{18}F-NaF	110 minutes	PET	Chemisorption onto hydroxypatite
^{18}F-FDG	110 minutes	PET	Glucose analog
^{11}C-choline	20.3 minutes	PET	Lipid-metabolism agent associated with overexpression of choline kinase
^{18}F-choline	110 minutes	PET	Lipid-metabolism agent associated with overexpression of choline kinase
^{11}C-acetate	20.3 minutes	PET	Lipid-metabolism agent associated with overexpression of fatty acid synthase
^{111}In-capromab pendetide	67 hours	Planar/SPECT	Antibody-based PSMA agent
Emerging PET agents			
^{18}F-FACBC	110 minutes	PET	L-Leucine analog amino acid transporter
^{18}F-FDHT	110 minutes	PET	Androgen analog targets androgen receptor
^{64}Cu-J591	13 hours	PET	Antibody-based PSMA agent
^{89}Zr-DFO-J591	78 hours	PET	Antibody-based PSMA agent
^{18}F-DCFBC	110 minutes	PET	Low-molecular-weight urea-based PSMA inhibitor
^{68}Ga-PSMA	68 minutes	PET	Low-molecular-weight urea-based PSMA inhibitor
Promising PET agents in development			
^{18}F-DCFPyL	110 minutes	PET	Low-molecular-weight PSMA-targeting agent
^{89}Zr-5A20	78 hours	PET	Free PSA-targeting agent
^{99m}Tc-RP527 (bombesin)	6 hours	SPECT	Gastrin-releasing peptide receptor
^{64}Cu-CB-TE2A-AR06 (bombesin)	13 hours	PET	Gastrin-releasing peptide receptor
^{124}I-CLR-1404	4 days	PET	Phospholipid ether analog/imaging
^{131}I-CLR-1404	8 days	SPECT	Phospholipid ether analog/therapy
^{18}F-glutamate/glutamine	110 minutes	PET	Glutamine analog

Abbreviations: PET, positron-emission tomography; MDP, methylene diphosphonate; FDG, fluorodeoxyglucose; FACBC, anti-1-amino-3-18F-fluorocyclobutane-1-carboxylic acid; FDHT, 16β-fluoro-5α-dihydrotestosterone; DFO, desferrioxamine B; DCFBC, *N*-[*N*-[(*S*)-1,3-dicarboxypropyl]carbamoyl]-4-fluorobenzyl-L-cysteine; PSMA, prostate-specific membrane antigen; ^{18}F-DCFPyL, 2-(3-[1-carboxy-5-[(6-[^{18}F]fluoropyridine-3-carbonyl)amino]pentyl]-ureido)pentanedioic acid; CB-TE2A-AR06, 4,11-bis(carboxymethyl)-1,4,8,11-tetraazabicyclo(6.6.2)hexadecane)-PEG_4-D-Phe-Gln-Trp-Ala-Val-Gly-His-Sta-Leu-NH_2; SPECT, single-photon-emission tomography; PSA, prostate-specific antigen.

Current imaging techniques

Traditional anatomic imaging

Conventional approaches for anatomic imaging of prostate cancer include transrectal ultrasound, computed tomography (CT), and magnetic resonance imaging (MRI). The use of transrectal ultrasound for detection of prostate cancer is limited, but it has an essential role in guidance for such interventions as prostate biopsies and radioactive seed placement in primary prostate cancer, as well as for evaluating local recurrence after radical prostatectomy in patients with increasing PSA serum levels.[5] CT is commonly used for initial staging of intermediate- to high-risk disease, to evaluate pelvic lymphadenopathy and extraprostatic disease extension. However, its sensitivity for detection of nodal metastases is only approximately 35%.[6] MRI has many potential applications in prostate cancer, including initial staging, biopsy guidance, surgical planning, radiation planning, and restaging after PSA relapse.[7] Standard anatomic imaging with CT and MRI has limited sensitivity and specificity for detection of primary prostate cancer, and other imaging methods are needed for this purpose. Multiparametric MRI, including diffusion-weighted imaging, dynamic contrast-enhanced MRI, and MR spectroscopy, however, are being found to be very helpful for detection and local staging of untreated prostate cancer, revealing such features as capsular and seminal vesicle invasion, thus discriminating patients with operable disease, or detecting residual or local recurrent prostate cancer.[8]

^{99m}Tc-MDP

Prostate cancer most frequently metastasizes to bones with predominantly osteoblastic (sclerotic) metastases. Therefore, the mainstay of imaging for advanced prostate cancer is technetium-99m-labeled bisphosphonate (eg, ^{99m}Tc-methylene diphosphonate [MDP]) bone scintigraphy, which is based on the incorporation of the bisphosphonate analog into hydroxyapatite crystals and collagen matrix. This molecular imaging technique is used for initial staging of intermediate- to high-risk disease and for restaging after PSA relapse. It is sensitive and can be used to survey the entire skeleton with a simple planar scan.[6] However, it has limited specificity and is not sensitive enough to detect smaller micrometastases. Single-photon-emission tomography (SPECT) and SPECT/CT have been shown to improve sensitivity in prostate cancer.[9,10] Quantitative analysis using the bone scan index has recently been shown to be prognostic for survival, and it is under investigation for assessment of treatment response.[11,12]

^{18}F-NaF

^{18}F-NaF is a diagnostic molecular imaging agent that is used for identification of new bone formation with PET imaging. The uptake mechanism of NaF resembles that of MDP, with better pharmacokinetic characteristics, including very rapid blood clearance, which results in a high bone-to-background ratio and twofold-higher uptake in bone compared to MDP.[13,14] It has been demonstrated that NaF PET is more sensitive than MDP planar bone scans or SPECT for prostate cancer bone metastases, and incorporation of bone findings from CT with PET/CT results in improved specificity.[9] Figure 2 demonstrates an example of prostate cancer metastases seen on NaF PET compared to an MDP bone scan. Another advantage of NaF PET is the shorter scan time, typically less than 1 hour, compared with a bone scan, resulting in a more efficient workflow, and improved patient convenience. NaF is one of the early skeletal scintigraphy agents, and was approved by the US Food and Drug Administration (FDA) in 1972; however, it was displaced by the arrival of MDP, which provided better resolution. However, with the widespread availability of

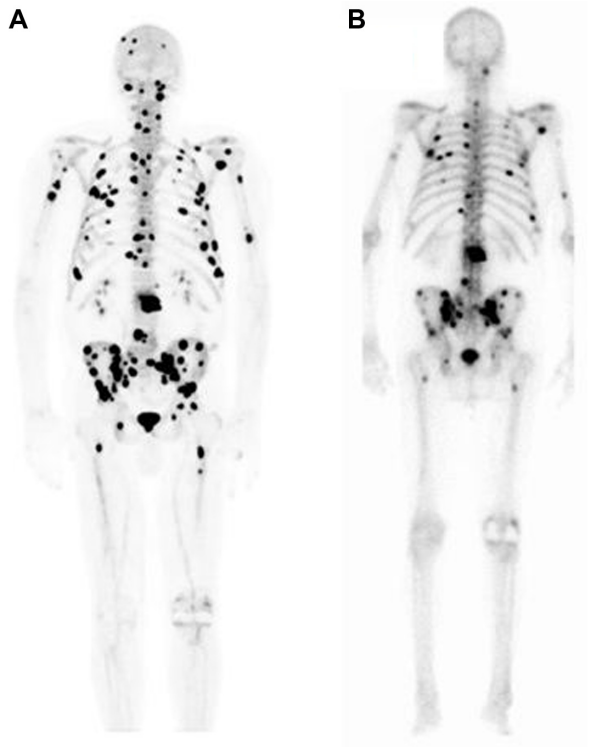

Figure 2 ^{18}F-NaF PET maximum-intensity projection for a 72-year-old patient with castration-resistant prostate cancer, showing innumerable osseous metastases throughout the skeleton (**A**). Note that multiple lesions were not identified on the same patient's ^{99m}Tc-MDP bone scan (**B**) performed 10 days before the ^{18}F-NaF PET scan, but showed fewer metastatic sites (University of Wisconsin PET Center).
Abbreviation: PET, positron-emission tomography.

high-quality PET scanners and the improved logistics for the delivery of ^{18}F-radiopharmaceuticals, prior logistical and technical limitations to the routine clinical use of NaF PET bone imaging have largely been overcome. At present, NaF PET typically is not performed routinely for clinical use outside large medical centers because of reimbursement issues, but a Center for Medicare and Medicaid Services National Oncologic PET Registry NaF coverage with evidence-development study is currently being performed to evaluate expansion of coverage for NaF for assessing bone metastatic disease.[15]

^{18}F-FDG

^{18}F-fluorodeoxyglucose (FDG) PET is an analog of glucose that reflects local rates of glucose consumption by tissues, and shows increased trapping by tumor cells due to increased metabolism and thus glycolytic activity of tumors.[16] FDG has been by far the most widely used agent for PET imaging for staging and restaging of most cancers.[17] However, it is limited in primary prostate cancer detection, due to slow growth and low glucose metabolism in early disease, compounded by artifacts created from high bladder activity due to urinary FDG accumulation.[18] In addition, FDG demonstrates nonspecific uptake in prostatitis and benign prostatic hypertrophy (BPH). A study by Hofer et al showed no difference between the ^{18}F-FDG uptake of benign prostate hyperplasia, prostate carcinoma, postoperative scar, or local recurrence after radical prostatectomy.[18] However, FDG PET can potentially play an important role in more advanced prostate cancer states. It has been shown to be most useful for evaluating lymph-node and bone metastases, given that it can image the soft tissue and bone simultaneously and provide a quantifiable expression of change using the standardized uptake value.[19] FDG PET may be useful for restaging after PSA relapse and for assessment of treatment response in CRPC.[16,19–21] A recent study by Meirelles et al showed that FDG PET was more sensitive than MDP bone scans for bone metastases as a result of CRPC.[22]

^{11}C/^{18}F-choline and ^{11}C-acetate

Prostate cancer cells rely more on fatty acid metabolism than glycolysis with upregulation and increased activity of lipogenic enzymes.[23] The ^{11}C/^{18}F choline-based (^{11}C/^{18}F-choline) and ^{11}C-acetate agents are lipid-metabolism PET agents that have been associated with overexpression of choline kinase[24,25] and fatty acid synthase,[26] respectively, in prostate cancer. ^{11}C/^{18}F-choline are taken up in prostate cancer cells through choline transporters and phosphorylated intracellularly by choline kinase.[27] An example of prostate cancer metastatic disease detection by ^{18}F-choline (^{18}F-FCH) PET/CT is shown in Figure 3. Acetate is incorporated into the membrane lipids due to overexpression of fatty acid synthase. The role of these agents in initial staging is not well established, because of false positives in prostatitis and BPH and false negatives in small (<5 mm) or necrotic tumors.[28] However, they have promising results for restaging after PSA relapse, with high sensitivity for local recurrence, nodal metastases, and bone metastases.[29–31] It is worth mentioning that ^{11}C-choline has been approved for use only at the Mayo Clinic by the FDA for restaging after PSA relapse.[31–33] Direct comparison of ^{11}C-acetate and ^{11}C-choline by Kotzerke et al revealed no clear clinical differences between these agents.[34]

A recent systematic review of the literature with meta-analysis of ^{11}C-acetate PET imaging in prostate cancer was done by Beheshti et al.[35] For primary tumor detection, pooled diagnostic indices were suboptimal: sensitivity of 75.1% (range: 69.8%–79.8%), and specificity of 75.8% (range: 72.4%–78.9%). This is because of the inability of ^{11}C-acetate PET imaging to show detect small subcentimeter nodal metastases and high uptake of this radiotracer at sites of BPH that overlapped with prostate cancer uptake. For detection of recurrent tumors, pooled sensitivity was 64% (59%–69%) and specificity of 93% (83%–98%), with higher sensitivity in patients with PSA levels >1 ng/mL and in postprostatectomy compared with external beam radiation therapy patients. Studies comparing ^{11}C-acetate-based and choline-based PET imaging were reported to be comparable in their analyses, with low sensitivity and relatively high specificity for detection of tumor recurrence and limited value for detection of primary tumors.[34,35]

In summary, although the available evidence indicates that choline- and acetate-based PET has analytic validity in subsets of patients, proof of clinical validity and clinical utility still must be provided.[36]

Emerging PET imaging agents

^{18}F-FACBC

Amino acids, such as leucine, methionine, and glutamine, are effectively taken up by many tumors because of increased amino acid transport and metabolism. The most promising of these agents for prostate cancer imaging is anti-1-amino-3-^{18}F-fluorocyclobutane-1-carboxylic acid (anti-^{18}F-FACBC or ^{18}F-FACBC), an L-leucine analog whose uptake is related to the activity of two amino acid transporters (ASC and LAT1), which appear to be upregulated in prostate cancer.[37,38]

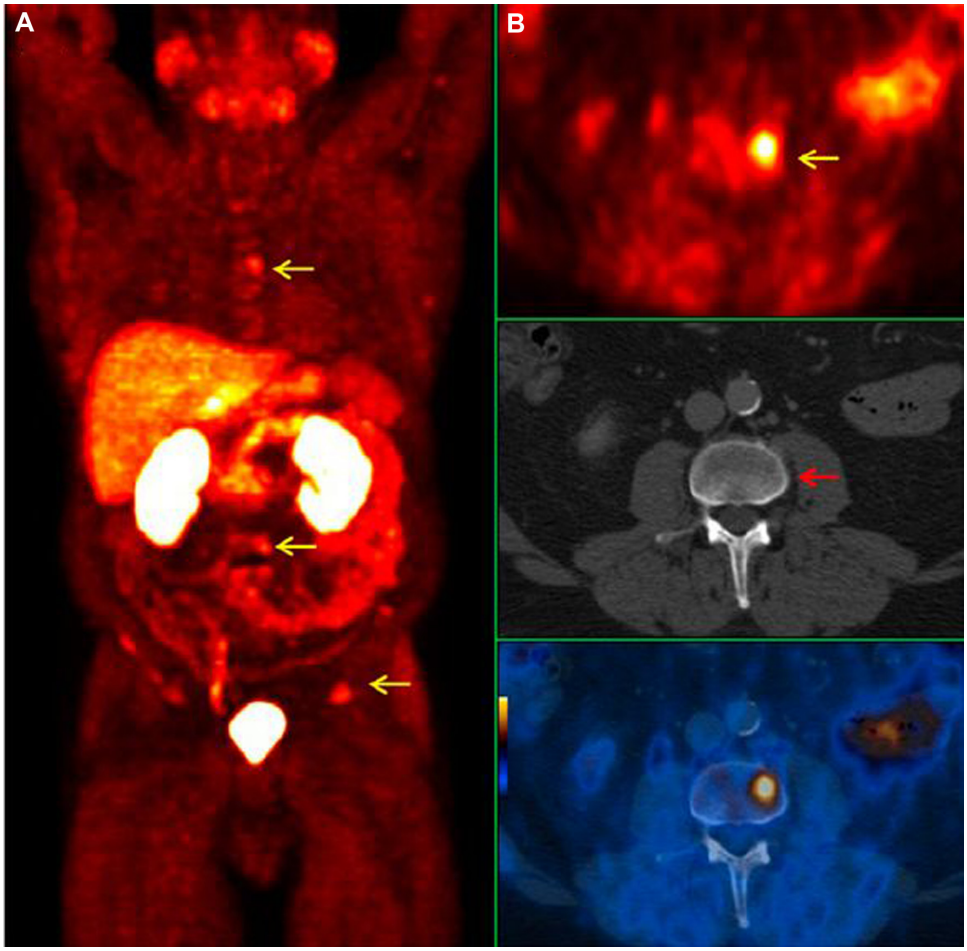

Figure 3 ^{18}F-choline (^{18}F-FCH) PET/CT images for a 64-year-old prostate cancer patient with a Gleason score of 7 and rising prostate-specific antigen. (**A**) PET maximum-intensity projection showing several foci of increased ^{18}F-FCH uptake correlates with osseous metastases (arrows). (**B**) Transaxial images showing increased ^{18}F-FCH uptake within L3 (yellow arrow), representing early bone marrow metastasis with no morphologic changes on CT (red arrow).
Note: This research was originally published in the *Journal of Nuclear Medicine*. Beheshti M, Haim S, Zakavi R, et al. Impact of 18F-choline PET/CT in prostate cancer patients with biochemical recurrence: influence of androgen deprivation therapy and correlation with PSA kinetics. *J Nucl Med*. 2013;54(6):833–840. © by the Society of Nuclear Medicine and Molecular Imaging, Inc.[27]
Abbreviations: PET, positron-emission tomography; CT, computed tomography.

^{18}F-FACBC has shown excellent prostate cancer-tumor uptake, with its normal biodistribution favorable for evaluating prostate cancer.[39] Normal uptake is found in the pancreas, liver, and bone marrow, with negligible uptake in the kidneys and very little urinary excretion. An advantage of ^{18}F-FACBC is a relatively long half-life of 109 minutes of an ^{18}F radiotracer compared to ^{11}C-choline or ^{11}C-acetate, which allows PET imaging without an onsite cyclotron.[40] This agent has shown early clinical success in imaging primary and recurrent prostate cancer (prostate bed, lymph nodes and bone metastases), with improved sensitivity compared with ^{111}In-capromab pendetide.[41–43] Schuster et al performed a prospective study on 50 patients with recurrent prostate cancer, comparing anti-3-^{18}F-FACBC PET/CT with ^{111}In-capromab pendetide SPECT/CT, and demonstrated encouraging results for anti-3-^{18}F-FACBC, which showed a sensitivity of 89%, specificity of 69%, and accuracy of 83%.[44] An example of primary cancer detection by ^{18}F-FACBC is shown in Figure 4.

^{18}F-FDHT

^{18}F-16β-fluoro-5α-dihydrotestosterone (FDHT) is an androgen analog that is an emerging agent for direct imaging of androgen receptors in prostate cancer.[45,46] A preclinical study by Bonasera et al[47] showed that FDHT accumulates avidly in the prostate gland of nonhuman primates and has a high binding affinity and selectivity for androgen receptors, and that this uptake was blocked by administration of testosterone. A prospective early study by Dehdashti et al[45] on 20 men with advanced prostate cancer demonstrated that metastatic and recurrent prostate cancer lesions can be detected by PET with FDHT with a sensitivity on a patient-by-patient basis of 63% and on

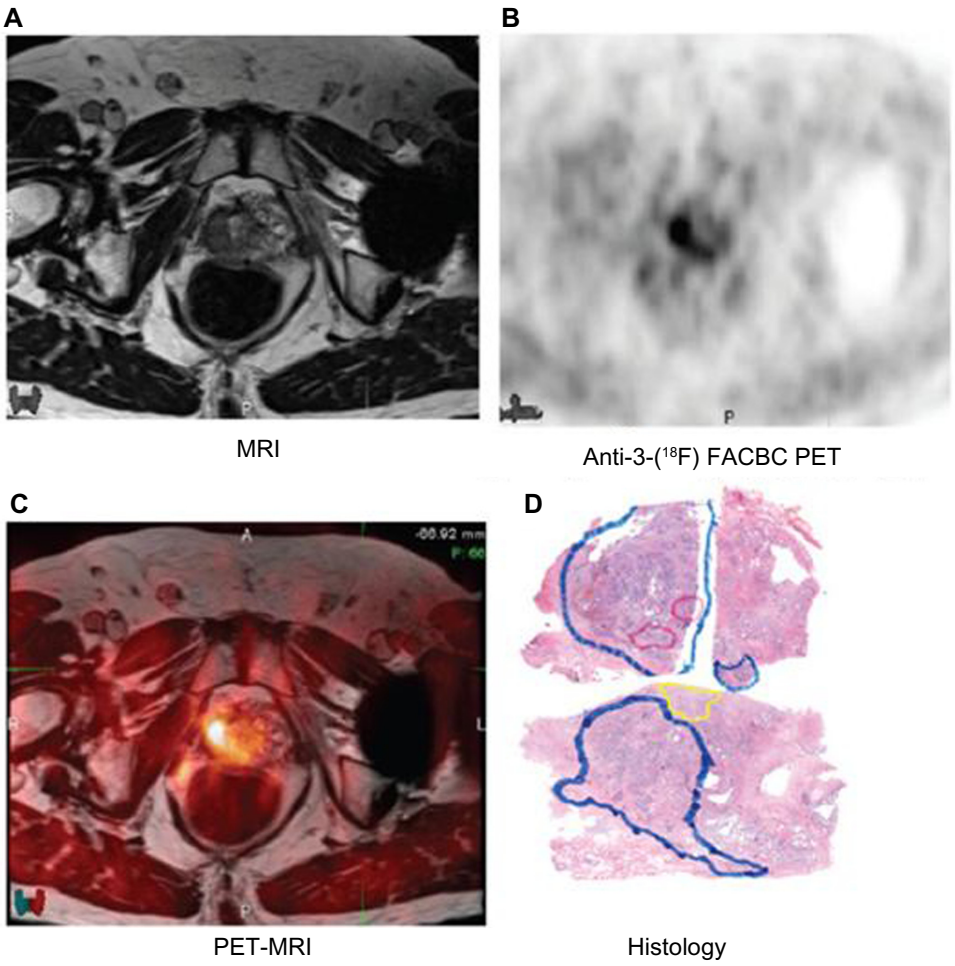

Figure 4 Primary prostate cancer detection by ^{18}F-FACBC. MRI (**A**), ^{18}F-FACBC PET (**B**), and coregistered PET/MRI (**C**) showing right anterior and posterior prostate ^{18}F-FACBC PET uptake that correlates with a tumor focus. On the histology (**D**), blue represents Gleason 4, red represents Gleason 5, and yellow represents benign prostatic hypertrophy.

Note: Reproduced with permission from Schuster DM, Taleghani PA, Nieh PT, et al. Characterization of primary prostate carcinoma by anti-1-amino-2-[(18)F]-fluorocyclobutane-1-carboxylic acid (anti-3-[(18)F] FACBC) uptake. *Am J Nucl Med Mol Imaging*. 2013;3(1):85–96.[41]

Abbreviations: MRI, magnetic resonance imaging; FACBC, ^{18}F-FACBC, anti-1-amino-3-^{18}F-fluorocyclobutane-1-carboxylic acid; PET, positron-emission tomography.

a lesion-by-lesion basis of 86%. A comparison of ^{18}F-FDHT and ^{18}F-FDG PET in prostate cancer metastases is shown in Figure 5. They also showed definite reduction in FDHT uptake in all lesions after patients had been treated with the antiandrogen drug flutamide. In another more recent study by Scher et al,[48] PET imaging of 22 patients revealed reduced FDHT binding after 4 weeks of enzalutamide therapy compared with baseline. This serves as proof of principle for application of molecular imaging agents for prostate cancer drug development and for assessment of individual treatment response.[16,45,46]

PSMA agents

Several molecular imaging agents have been developed to target the biomarker prostate-specific membrane antigen (PSMA), an integral membrane glycoprotein that is upregulated in prostate cancer, particularly in advanced, hormone-independent, and metastatic disease, and is an active target for the development of imaging agents for prostate cancer.[49,50]

PSMA is expressed in the prostate at a level of 1,000-fold greater than in other tissues, and eight- to 12-fold higher in prostate cancer over the noncancerous prostate,[51] particularly in high-grade, hormone-independent, and metastatic disease. These features of PSMA make it an optimal target for developing imaging and therapy strategies for prostate cancer. PSMA agents can be classified into antibodies and antibody fragments and low-molecular-weight compounds that include two types: ureas and phosphoramidates.[52]

Antibody-based PSMA agents

The first imaging method using PSMA as an antigen target was the antibody capromab pendetide (ProstaScint®), which

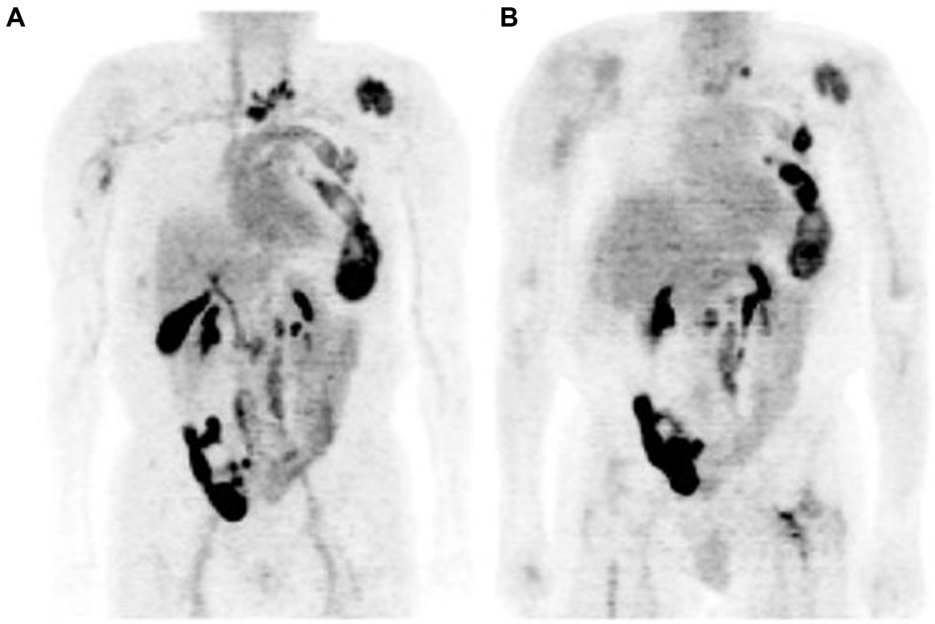

Figure 5 ^{18}F-FDHT PET. Comparison of (**A**) ^{18}F-FDHT and (**B**) ^{18}F-FDG PET scans in maximum-intensity projection views with widespread bone metastases involving cervical spine, left ribs, and left para-aortic lymph nodes and physiological urinary activity in a right lower abdominal quadrant urinary diversion.
Note: This research was originally published in JNM. Larson SM, Morris M, Gunther I, et al. Tumor localization of 16β-18F-fluoro-5α-dihydrotestosterone versus 18F-FDG in patients with progressive, metastatic prostate cancer. *J Nucl Med.* 2004;45(3):366–373. © by the Society of Nuclear Medicine and Molecular Imaging, Inc.[46]
Abbreviations: FDHT, 16β-fluoro-5α-dihydrotestosterone; FDG, fluorodeoxyglucose; PET, positron-emission tomography.

is labeled by ^{111}In (^{111}In-capromab pendetide), and is the only PSMA-based imaging agent that has gained FDA approval to date.[53] Clinical evaluation of ^{111}In-capromab pendetide for detection of prostate cancer recurrence outside the prostate fossa in the biochemical recurrence setting has been disappointing, and overall has been of limited clinical utility for prostate cancer management.[54] Some of the issues inherent with the limitation of this agent are the targeting of the internal epitope of PSMA and the use of an intact antibody that has prolonged blood-pool retention, leading to high background signals and subsequently reduced detection rates, as well as the inherently lower spatial resolution of ^{111}In planar and SPECT scintigraphic techniques when compared to PET.[55] Furthermore, results obtained with ProstaScint have been controversial, with some reports claiming no advantage in using the scan in patients with rising PSA postprostatectomy.[56]

Second- and third-generation humanized PSMA-binding antibodies have been more successful at targeting this promising prostate cancer biomarker. Humanized monoclonal antibody J591 demonstrated superior targeting compared with capromab pendetide, due to targeting of the extracellular epitope of PSMA, with excellent binding characteristics and tumor-to-background ratio in prostate cancer xenografts.[50] One of the J591-based agents is ^{64}Cu-J591, which has been studied in animals but not in humans, and demonstrated PSMA upregulation after androgen blockade.[33] Recent success in imaging with ^{89}Zr-labeled J591 has been observed in preclinical models, with excellent tumor uptake and retention by the PET agent ^{89}Zr-desferrioxamine B (DFO)-J591 (^{89}Zr-J591).[57] The first report of ^{89}Zr-J591 PET in localized prostate cancer cases was reported by Osborne et al[58] in 2013. In this pilot study on eleven patients, they found that ^{89}Zr-J591 bound to tumor foci in situ and PET identified primarily Gleason score 7 or greater and larger tumors, likely corresponding to clinically significant disease warranting definitive therapy. Results from another recent pilot study were reported by Pandit-Taskar et al[59] in ten patients to evaluate biodistribution, kinetics, radiation dosimetry and lesion detectability by ^{89}Zr-J591, and showed excellent targeting of prostate cancer lesions. They reported that all ^{89}Zr-J591-positive lesions were histologically confirmed as prostate cancer, and a nodal disease in two patients was identified by this imaging method only, whereas other imaging (FDG PET and CT) was negative.

Low molecular weight-based PSMA agents

^{18}F-DCFBC

A low-molecular-weight, urea-based inhibitor of PSMA, ^{18}F-*N*-[*N*-[(*S*)-1,3-dicarboxypropyl]carbamoyl]-4-fluorobenzyl-L-cysteine (^{18}F-DCFBC) was the first agent for low-molecular-weight PSMA-targeted PET imaging of

prostate cancer.[56] Initial preclinical studies in prostate cancer mouse-xenograft studies by Mease et al[56] demonstrated high tumor-to-background ratio and rapid clearance from nontarget sites, with a target-to-background ratio of 20:1 at 120 minutes after injection. The time-activity curves indicated that ^{18}F-DCFBC had achieved equilibrium by 120 minutes, and had begun to decrease in concentration at the target site. It has been developed and evaluated in a first-in-human clinical trial for progressive metastatic prostate cancer.[60] Bone and soft-tissue metastases were successfully visualized by ^{18}F-DCFBC PET, as also were probable early bone lesions that were not seen on CT or MDP bone scans.[60] Figure 6 demonstrates bone and nodal metastatic disease detection by ^{18}F-DCFBC PSMA PET. These early promising results, in conjunction with appropriate pharmacokinetics and dosimetry, lay the groundwork for further evaluation in larger prospective clinical trials of ^{18}F-DCFBC as a prostate cancer PET imaging agent.

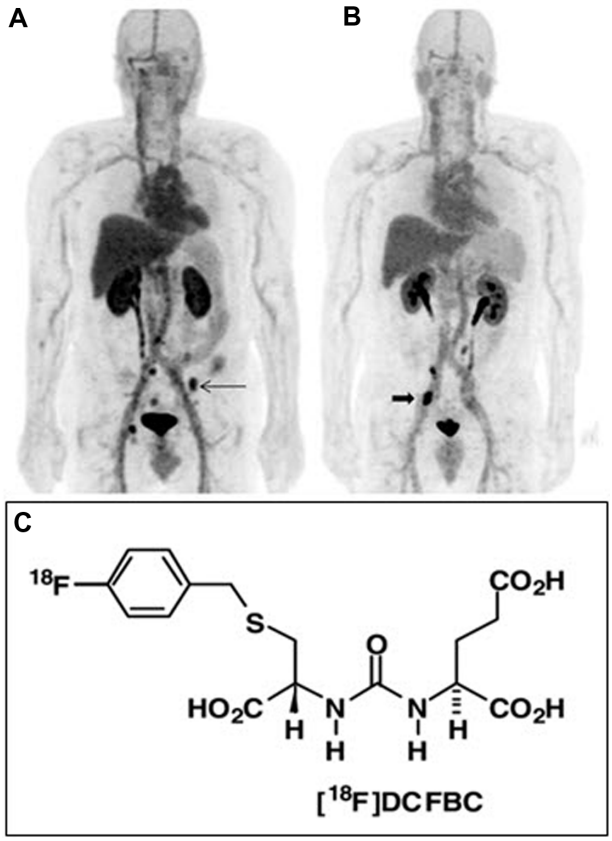

Figure 6 ^{18}F-DCFBC PSMA-based PET. ^{18}F-DCFBC prostate-specific membrane antigen-based PET maximum-intensity projection images demonstrating patients with multiple bone metastases (**A**) and lymph node metastases (**B**). The chemical structure of ^{18}F-DCFBC (**C**).
Note: This research was originally published in JNM. Cho SY, Gage KL, Mease RC, et al. Biodistribution, tumor detection, and radiation dosimetry of 18F-DCFBC, a low-molecular-weight inhibitor of prostate-specific membrane antigen, in patients with metastatic prostate cancer. *J Nucl Med.* 2012;53(12):1883–1891. © by the Society of Nuclear Medicine and Molecular Imaging, Inc.[60]
Abbreviations: DCFBC, *N*-[*N*-[(*S*)-1,3-dicarboxypropyl]carbamoyl]-4-fluorobenzyl-L-cysteine; PET, positron-emission tomography.

^{68}Ga-PSMA

Another urea-based inhibitor of PSMA, Glu-NH-CO-NH-Lys-(Ahx)-[^{68}Ga(HBED-CC)] (^{68}Ga-PSMA) is another promising low-molecular-weight PSMA-based imaging PET agent. Afshar-Oromieh et al[55] evaluated the biodistribution and tumor uptake of ^{68}Ga-PSMA in 37 patients, and showed excellent contrast between tumor lesions and background as early as 1 hour postinjection, with high detection rates even at low PSA levels. Later images at 3 hours showed better contrast, with a median tumor-to-background ratio of 28:1. Another recent study comparing ^{68}Ga-PSMA with ^{18}F-fluorocholine with biochemical relapse of prostate cancer in 37 patients within a 10-day time window was able to detect more lesions and higher signal-to-background noise using ^{68}Ga-PSMA compared with ^{18}F-fluorocholine (78 versus 56, respectively; P=0.04).[61]

Promising PET imaging agents in development

^{18}F-DCFPyL

A second-generation low-molecular-weight ^{18}F-fluorine-labeled PSMA targeting agent, 2-(3-[1-carboxy-5-[(6-[^{18}F]fluoropyridine-3-carbonyl)amino]pentyl]-ureido)pentanedioic acid (^{18}F-DCFPyL), has also been developed to improve tumor uptake and clearance from nontarget sites. Preclinical studies have demonstrated a high tumor-to-background ratio at 2 hours postinjection of 39.4%±5.4% injected dose (ID)/g within PSMA-expressing tumor xenografts.[49,62] An animal study on mice by Chen et al[63] showed high and prolonged PSMA-selective uptake, with very low nontarget uptake and rapid clearance from normal organs. They demonstrated that the uptake in PSMA$^+$ PC-3 PIP tumor was 46.7%±5.8% ID/g at 30 minutes postinjection and 36.6%±4.3% ID/g at 4 hours. A first-in-man clinical trial of this radiotracer is currently being conducted at Johns Hopkins University.

Free prostate-specific antigen imaging

A novel radiotracer that targets free PSA, ^{89}Zr-labeled 5A10 has been developed and studied preclinically by Ulmert et al.[64] They demonstrated that ^{89}Zr-5A10 is localized to multiple androgen receptor- and PSA-positive prostate cancer models, with a decline in free PSA synthesis induced by antiandrogen therapy in a clinically validated xenograft model of CRPC. This new radiotracer may offer more accurate staging, given

it specifically targets prostate cancer osseous metastases rather than nonmalignant skeletal pathologies, unlike bone scintigraphy, which is less specific. However, one of the limitations of ^{89}Zr-5A10 in prostate cancer is overexpression of PSA also in benign pathologies of the prostate; therefore, local detection of primary prostate cancer might be challenging.

Bombesin-based agents

Bombesin-like peptides, such as gastrin-releasing peptide (GRP), have been shown to play a role in oncology. The GRP receptor (GRPr), a member of the bombesin-receptor family, is physiologically expressed in the gastrointestinal tract and central nervous system, and is found to be overexpressed in different malignant tumors, but most consistently in prostate cancer. Therefore, it is considered a promising target for sensitive and specific imaging target for prostate cancer.[65] A study by Markwalder and Reubi[66] on 50 patients with primary prostate cancer or primary urinary bladder cancer demonstrated high density of GRPrs not only in invasive prostatic carcinomas but also in prostatic intraepithelial neoplasia. This is in contrast to an absence or low density of GRPrs in nonneoplastic prostatic tissue, in particular benign prostatic hyperplasia.

Different bombesin-receptor ligands have been tested preclinically, but a limited number of these have been evaluated in humans. An example is the ^{99m}Tc-labeled bombesin agonist ^{99m}Tc-RP527, tested in patients with breast and prostate cancers, which however showed some limitation due to high gastrointestinal uptake, which may limit the detection of metastatic prostate cancer. GRPr antagonists were studied in preclinical models of prostate cancer, and showed higher tumor uptake and lower gastrointestinal uptake than the agonists. One of the studied GRPr antagonists, ^{64}Cu-CB-TE2A-AR06 [(^{64}Cu-4,11-bis(carboxymethyl)-1,4,8,11-tetraazabicyclo(6.6.2)hexadecane)-PEG$_4$-D-Phe-Gln-Trp-Ala-Val-Gly-His-Sta-Leu-NH$_2$], demonstrated the most favorable tumor uptake and tumor-to-background contrast. A recent pilot clinical study by Wieser et al[65] on four patients with newly diagnosed prostate cancer without prior therapy showed favorable biodistribution and high tumor uptake of GRPr antagonists that were rapidly cleared from organs with physiologic GRPr expression and retained significantly longer in human prostate cancers, with an example seen in Figure 7. This resulted in steadily increasing tumor-to-background ratios over time. Studies in a larger number of patients will be necessary in order to determine the sensitivity

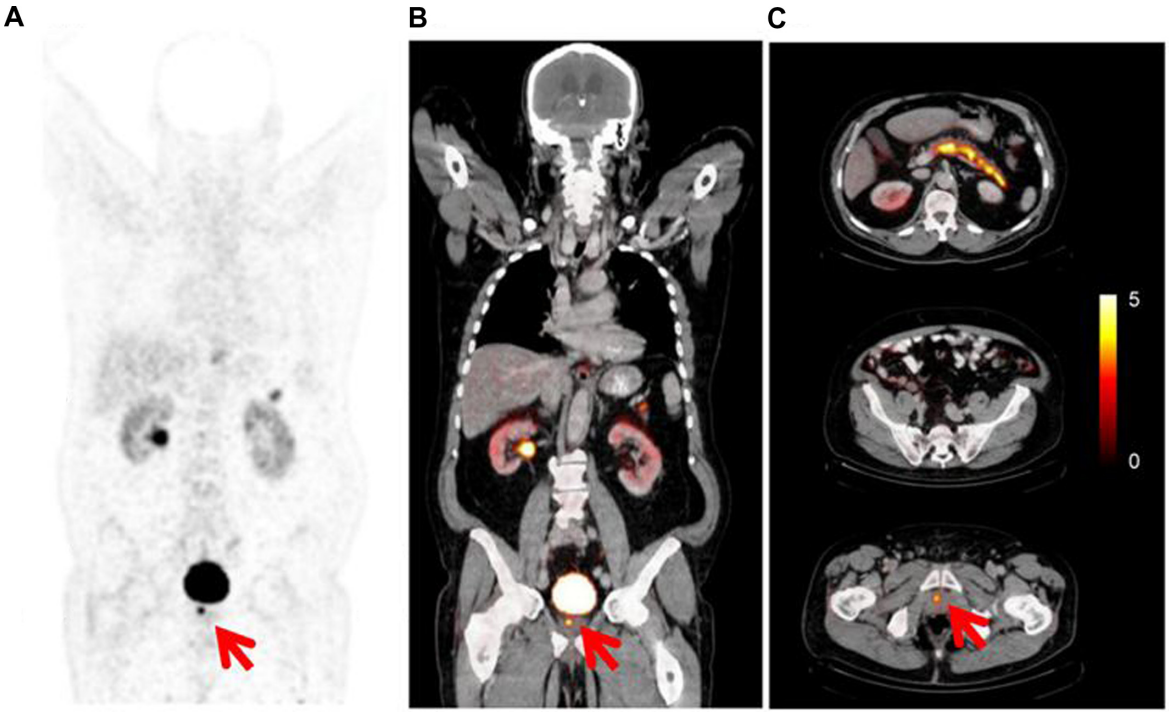

Figure 7 (**A**–**C**) PET/CT gastrin-releasing peptide-receptor or bombesin-receptor imaging with ^{64}Cu-CB-TE2A-AR06, showing focal uptake of primary prostate cancer (red arrows), below urinary bladder activity.

Abbreviations: PET, positron-emission tomography; CT computed tomography; CB-TE2A-AR06, 4,11-bis(carboxymethyl)-1,4,8,11-tetraazabicyclo(6.6.2)hexadecane)-PEG$_4$-D-Phe-Gln-Trp-Ala-Val-Gly-His-Sta-Leu-NH$_2$.

of ^{64}Cu-CB-TE2A-AR06 PET/CT. ^{68}Ga-based GRPr PET imaging radiotracers are also being developed.[65]

Phospholipid ether analogs

Counsell et al[67] and Pinchuk et al[68] have developed multiple radiolabeled versions of phospholipid ether analogs that enter malignant cells via overexpressed membrane-lipid rafts. One of the emerging phospholipid ether analogs is CLR1404, which has promising applications in oncology, including prostate cancer. Radioiodine labeling of this agent with ^{124}I and ^{131}I enables cancer imaging and therapy, respectively. This agent shows significant clearance from organs, with prolonged tumor retention for days to weeks postinjection, enabling excellent tumor-to-background ratios. In contrast to ^{18}F-FDG, CLR1404 shows minimal or even no physiologic uptake in the brain, which enables visualization of brain metastases with excellent contrast.[69]

A recent preliminary study by Pickhardt et al[70] on 22 patients with different solid tumors, including three patients with prostate cancer, showed preferential uptake of ^{124}I- and ^{131}I-labeled CLR1404 within a variety of metastatic foci, with persistent tumor retention coupled with progressive washout of background activity. Further clinical trials with this new agent are under way.

^{11}C/^{18}F-glutamate/glutamine

The amino acid glutamine is the most abundant nonessential amino acid in the human body, and has been recognized as an important tumor nutrient. Glutamine enters the cells via glutamine transporters and is converted by glutaminase to glutamate, leading to high intracellular concentrations of glutamate.[71,72] Since glutamine metabolism is upregulated in many tumors, using radiolabeled glutamine and its related derivatives in tumor imaging is appropriate. The ability of some tumors preferentially to use glutamine rather than glucose to satisfy their metabolic needs suggests that ^{18}F-FDG PET-negative tumors may have elevated rates of glutaminolysis. Several ^{11}C- and ^{18}F-labeled glutamine analogs have been used as PET tumor-imaging agents in humans.[73] An animal study by Qu et al[73] using ^{11}C-labeled glutamine (L-[5-^{11}C]-glutamine), showed maximum tumor uptake at 20 minutes after injection that remained consistent throughout the 60-minute scan time with little to no washout, suggesting that the radioactivity was taken up and trapped in the tumor tissue. ^{18}F-labeled glutamine analogs are now emerging for tumor imaging, including prostate cancer, which has a longer physical half-life (110 minutes) compared to ^{11}C-labeled glutamine analogs, and may provide a more convenient and useful tool for mapping glutamine metabolism.

Multimodality PET/MRI

Simultaneous acquisition of multiparametric MR and PET images has been recently introduced that incorporates the advantages of both PET and MRI together and offers simultaneous instead of sequential acquisitions. PET/MRI provides combined structural, metabolic, and functional imaging information with improved soft-tissue contrast and availability of sophisticated MRI sequences, such as diffusion and perfusion imaging, functional MRI, and MR spectroscopy. This in turn improves the accuracy in the detection and staging of untreated primary prostate cancer, and detection of residual or local recurrence. Furthermore, the use of PET/MRI would result in a significant decrease in radiation exposure.[9]

Conclusion

As management of prostate cancer is moving toward more personalized patient-adapted therapy, there is an increasing demand for more specialized molecular imaging beyond ^{99m}Tc-MDP scintigraphy. In this article, we have reviewed many existing and emerging molecular imaging agents for prostate cancer in different stages of development. Many of these agents have promising potential for more specific detection of primary and metastatic disease for facilitating a mechanism-based personalized approach to disease management.

Disclosure

The authors report no conflicts of interest in this work.

References

1. Jemal A, Siegel R, Xu J, Ward E. Cancer statistics, 2010. *CA Cancer J Clin*. 2010;60(5):277–300.
2. Thompson I, Thrasher JB, Aus G, et al. Guideline for the management of clinically localized prostate cancer: 2007 update. *J Urol*. 2007;177(6):2106–2131.
3. Crawford ED, Flaig TW. Optimizing outcomes of advanced prostate cancer: drug sequencing and novel therapeutic approaches. *Oncology (Williston Park)*. 2012;26(1):70–77.
4. Yap TA, Zivi A, Omlin A, de Bono JS. The changing therapeutic landscape of castration-resistant prostate cancer. *Nat Rev Clin Oncol*. 2011;8(10):597–610.
5. Shinohara K, Wheeler TM, Scardino PT. The appearance of prostate cancer on transrectal ultrasonography: correlation of imaging and pathological examinations. *J Urol*. 1989;142(1):76–82.
6. Hricak H, Choyke PL, Eberhardt SC, Leibel SA, Scardino PT. Imaging prostate cancer: a multidisciplinary perspective. *Radiology*. 2007;243(1):28–53.
7. Sciarra A, Barentsz J, Bjartell A, et al. Advances in magnetic resonance imaging: how they are changing the management of prostate cancer. *Eur Urol*. 2011;59(6):962–977.

8. Bonekamp D, Jacobs MA, El-Khouli R, Stoianovici D, Macura KJ. Advancements in MR imaging of the prostate: from diagnosis to interventions. *Radiographics*. 2011;31(3):677–703.
9. Even-Sapir E, Metser U, Mishani E, Lievshitz G, Lerman H, Leibovitch I. The detection of bone metastases in patients with high-risk prostate cancer: 99mTc-MDP planar bone scintigraphy, single- and multi-field-of-view SPECT, 18F-fluoride PET, and 18F-fluoride PET/CT. *J Nucl Med*. 2006;47(2):287–297.
10. Helyar V, Mohan HK, Barwick T, et al. The added value of multislice SPECT/CT in patients with equivocal bony metastasis from carcinoma of the prostate. *Eur J Nucl Med Mol Imaging*. 2010;37(4):706–713.
11. Dennis ER, Jia X, Mezheritskiy IS, et al. Bone scan index: a quantitative treatment response biomarker for castration-resistant metastatic prostate cancer. *J Clin Oncol*. 2012;30(5):519–524.
12. Ulmert D, Kaboteh R, Fox JJ, et al. A novel automated platform for quantifying the extent of skeletal tumour involvement in prostate cancer patients using the Bone Scan Index. *Eur Urol*. 2012;62(1):78–84.
13. Segall G, Delbeke D, Stabin MG, et al. SNM practice guideline for sodium 18F-fluoride PET/CT bone scans 1.0. *J Nucl Med*. 2010;51(11):1813–1820.
14. Grant FD, Fahey FH, Packard AB, Davis RT, Alavi A, Treves ST. Skeletal PET with 18F-fluoride: applying new technology to an old tracer. *J Nucl Med*. 2008;49(1):68–78.
15. Hillner BE, Siegel BA, Hanna L, et al. Impact of 18F-fluoride PET on Intended Management of Patients with Cancers Other Than Prostate Cancer: Results from the National Oncologic PET Registry. *J Nucl Med*. 2014;55(7):1054–1061.
16. Fox JJ, Schöder H, Larson SM. Molecular imaging of prostate cancer. *Curr Opin Urol*. 2012;22(4):320–327.
17. Shankar LK, Hoffman JM, Bacharach S, et al. Consensus recommendations for the use of 18F-FDG PET as an indicator of therapeutic response in patients in National Cancer Institute trials. *J Nucl Med*. 2006;47(6):1059–1066.
18. Hofer C, Laubenbacher C, Block T, Breul J, Hartung R, Schwaiger M. Fluorine-18-fluorodeoxyglucose positron emission tomography is useless for the detection of local recurrence after radical prostatectomy. *Eur Urol*. 1999;36(1):31–35.
19. Morris MJ, Akhurst T, Larson SM, et al. Fluorodeoxyglucose positron emission tomography as an outcome measure for castrate metastatic prostate cancer treated with antimicrotubule chemotherapy. *Clin Cancer Res*. 2005;11(9):3210–3216.
20. Chang CH, Wu HC, Tsai JJ, Shen YY, Changlai SP, Kao A. Detecting metastatic pelvic lymph nodes by 18F-2-deoxyglucose positron emission tomography in patients with prostate-specific antigen relapse after treatment for localized prostate cancer. *Urol Int*. 2003;70(4): 311–315.
21. Schöder H, Herrmann K, Gönen M, et al. 2-[18F]fluoro-2-deoxyglucose positron emission tomography for the detection of disease in patients with prostate-specific antigen relapse after radical prostatectomy. *Clin Cancer Res*. 2005;11(13):4761–4769.
22. Meirelles GS, Schöder H, Ravizzini GC, et al. Prognostic value of baseline [18F] fluorodeoxyglucose positron emission tomography and 99mTc-MDP bone scan in progressing metastatic prostate cancer. *Clin Cancer Res*. 2010;16(24):6093–6099.
23. Zadra G, Photopoulos C, Loda M. The fat side of prostate cancer. *Biochim Biophys Acta*. 2013;1831(10):1518–1532.
24. Contractor K, Challapalli A, Barwick T, et al. Use of [11C]choline PET-CT as a noninvasive method for detecting pelvic lymph node status from prostate cancer and relationship with choline kinase expression. *Clin Cancer Res*. 2011;17(24):7673–7683.
25. Henriksen G, Herz M, Hauser A, Schwaiger M, Wester HJ. Synthesis and preclinical evaluation of the choline transport tracer deshydroxy-[18F]fluorocholine ([18F]dOC). *Nucl Med Biol*. 2004;31(7):851–858.
26. Vavere AL, Kridel SJ, Wheeler FB, Lewis JS. 1-11C-acetate as a PET radiopharmaceutical for imaging fatty acid synthase expression in prostate cancer. *J Nucl Med*. 2008;49(2):327–334.
27. Beheshti M, Haim S, Zakavi R, et al. Impact of 18F-choline PET/CT in prostate cancer patients with biochemical recurrence: influence of androgen deprivation therapy and correlation with PSA kinetics. *J Nucl Med*. 2013;54(6):833–840.
28. Souvatzoglou M, Weirich G, Schwarzenboeck S, et al. The sensitivity of [11C]choline PET/CT to localize prostate cancer depends on the tumor configuration. *Clin Cancer Res*. 2011;17(11):3751–3759.
29. Castellucci P, Fuccio C, Nanni C, et al. Influence of trigger PSA and PSA kinetics on 11C-choline PET/CT detection rate in patients with biochemical relapse after radical prostatectomy. *J Nucl Med*. 2009;50(9):1394–1400.
30. Picchio M, Castellucci P. Clinical indications of C-choline PET/CT in prostate cancer patients with biochemical relapse. *Theranostics*. 2012;2(3):313–317.
31. Picchio M, Spinapolice EG, Fallanca F, et al. [11C]choline PET/CT detection of bone metastases in patients with PSA progression after primary treatment for prostate cancer: comparison with bone scintigraphy. *Eur J Nucl Med Mol Imaging*. 2012;39(1):13–26.
32. [No authors listed]. FDA approves 11C-choline for PET in prostate cancer. *J Nucl Med*. 2012;53(12):11N.
33. Kiess AP, Cho SY, Pomper MG. Translational molecular imaging of prostate cancer. *Curr Radiol Rep*. 2013;1(3):216–226.
34. Kotzerke J, Volkmer BG, Glatting G, et al. Intraindividual comparison of [11C]acetate and [11C]choline PET for detection of metastases of prostate cancer. *Nuklearmedizin*. 2003;42(1):25–30.
35. Beheshti M, Treglia G, Zakavi SR, et al. Application of 11C-acetate positron-emission tomography (PET) imaging in prostate cancer: systematic review and meta-analysis of the literature. *BJU Int*. 2013;112(8):1062–1072.
36. Umbehr MH, Müntener M, Hany T, Sulser T, Bachmann LM. The role of 11C-choline and 18F-fluorocholine positron emission tomography (PET) and PET/CT in prostate cancer: a systematic review and meta-analysis. *Eur Urol*. 2013;64(1):106–117.
37. Okudaira H, Shikano N, Nishii R, et al. Putative transport mechanism and intracellular fate of trans-1-amino-3-18F-fluorocyclobutanecarboxylic acid in human prostate cancer. *J Nucl Med*. 2011;52(5):822–829.
38. Oka S, Hattori R, Kurosaki F, et al. A preliminary study of anti-1-amino-3-18F-fluorocyclobutyl-1-carboxylic acid for the detection of prostate cancer. *J Nucl Med*. 2007;48(1):46–55.
39. Nye JA, Schuster DM, Yu W, Camp VM, Goodman MM, Votaw JR. Biodistribution and radiation dosimetry of the synthetic nonmetabolized amino acid analogue anti-18F-FACBC in humans. *J Nucl Med*. 2007;48(6):1017–1020.
40. Nanni C, Schiavina R, Rubello D, et al. The detection of disease relapse after radical treatment for prostate cancer: is anti-3-18F-FACBC PET/CT a promising option? *Nucl Med Commun*. 2013;34(9):831–833.
41. Schuster DM, Taleghani PA, Nieh PT, et al. Characterization of primary prostate carcinoma by anti-1-amino-2-[(18)F]-fluorocyclobutane-1-carboxylic acid (anti-3-[(18)F] FACBC) uptake. *Am J Nucl Med Mol Imaging*. 2013;3(1):85–96.
42. Amzat R, Taleghani P, Savir-Baruch B, et al. Unusual presentations of metastatic prostate carcinoma as detected by anti-3 F-18 FACBC PET/CT. *Clin Nucl Med*. 2011;36(9):800–802.
43. Schuster DM, Votaw JR, Nieh PT, et al. Initial experience with the radiotracer anti-1-amino-3-18F-fluorocyclobutane-1-carboxylic acid with PET/CT in prostate carcinoma. *J Nucl Med*. 2007;48(1):56–63.
44. Schuster DM, Savir-Baruch B, Nieh PT, et al. Detection of recurrent prostate carcinoma with anti-1-amino-3-18F-fluorocyclobutane-1-carboxylic acid PET/CT and 111In-capromab pendetide SPECT/CT. *Radiology*. 2011;259(3):852–861.
45. Dehdashti F, Picus J, Michalski JM, et al. Positron tomographic assessment of androgen receptors in prostatic carcinoma. *Eur J Nucl Med Mol Imaging*. 2005;32(3):344–350.
46. Larson SM, Morris M, Gunther I, et al. Tumor localization of 16β-18F-fluoro-5α-dihydrotestosterone versus 18F-FDG in patients with progressive, metastatic prostate cancer. *J Nucl Med*. 2004;45(3):366–373.

47. Bonasera TA, O'Neil JP, Xu M, et al. Preclinical evaluation of fluorine-18-labeled androgen receptor ligands in baboons. *J Nucl Med*. 1996;37(6):1009–1015.
48. Scher HI, Beer TM, Higano CS, et al. Antitumour activity of MDV3100 in castration-resistant prostate cancer: a phase 1-2 study. *Lancet*. 2010;375(9724):1437–1446.
49. Foss CA, Mease RC, Cho SY, Kim HJ, Pomper MG. GCPII imaging and cancer. *Curr Med Chem*. 2012;19(9):1346–1359.
50. Osborne JR, Akhtar NH, Vallabhajosula S, Anand A, Deh K, Tagawa ST. Prostate-specific membrane antigen-based imaging. *Urol Oncol*. 2013;31(2):144–154.
51. O'Keefe DS, Bacich DJ, Heston WD. Comparative analysis of prostate-specific membrane antigen (PSMA) versus a prostate-specific membrane antigen-like gene. *Prostate*. 2004;58(2):200–210.
52. Eder M, Eisenhut M, Babich J, Haberkorn U. PSMA as a target for radiolabelled small molecules. *Eur J Nucl Med Mol Imaging*. 2013;40(6):819–823.
53. Bander NH. Technology insight: monoclonal antibody imaging of prostate cancer. *Nat Clin Pract Urol*. 2006;3(4):216–225.
54. Thomas CT, Bradshaw PT, Pollock BH, et al. Indium-111-capromab pendetide radioimmunoscintigraphy and prognosis for durable biochemical response to salvage radiation therapy in men after failed prostatectomy. *J Clin Oncol*. 2003;21(9):1715–1721.
55. Afshar-Oromieh A, Malcher A, Eder M, et al. PET imaging with a [68Ga]gallium-labelled PSMA ligand for the diagnosis of prostate cancer: biodistribution in humans and first evaluation of tumour lesions. *Eur J Nucl Med Mol Imaging*. 2013;40(4):486–495.
56. Mease RC, Dusich CL, Foss CA, et al. N-[N-[(S)-1,3-Dicarboxypropyl] carbamoyl]-4-[18F]fluorobenzyl-L-cysteine, [18F]DCFBC: a new imaging probe for prostate cancer. *Clin Cancer Res*. 2008;14(10):3036–3043.
57. Holland JP, Divilov V, Bander NH, Smith-Jones PM, Larson SM, Lewis JS. 89Zr-DFO-J591 for immunoPET of prostate-specific membrane antigen expression in vivo. *J Nucl Med*. 2010;51(8):1293–1300.
58. Osborne JR, Green DA, Spratt DE, et al. A prospective pilot study of (89)Zr-J591/prostate specific membrane antigen positron emission tomography in men with localized prostate cancer undergoing radical prostatectomy. *J Urol*. 2014;191(5):1439–1445.
59. Pandit-Taskar N, O'Donoghue J, Beylergil V, et al. 89Zr J591 immuno-PET imaging in patients with prostate cancer. *Eur J Nucl Med Mol Imaging*. 2014;41(11):2093–2105.
60. Cho SY, Gage KL, Mease RC, et al. Biodistribution, tumor detection, and radiation dosimetry of 18F-DCFBC, a low-molecular-weight inhibitor of prostate-specific membrane antigen, in patients with metastatic prostate cancer. *J Nucl Med*. 2012;53(12):1883–1891.
61. Afshar-Oromieh A, Zechmann CM, Malcher A, et al. Comparison of PET imaging with a Ga-labelled PSMA ligand and F-choline-based PET/CT for the diagnosis of recurrent prostate cancer. *Eur J Nucl Med Mol Imaging*. 2014;41(1):11–20.
62. Mease RC, Foss CA, Pomper MG. PET imaging in prostate cancer: focus on prostate-specific membrane antigen. *Curr Top Med Chem*. 2013;13(8):951–962.
63. Chen Y, Pullambhatla M, Foss CA, et al. 2-(3-{1-Carboxy-5-[(6-[18F] fluoro-pyridine-3-carbonyl)-amino]-pentyl}-ureido)-pen tanedioic acid, [18F]DCFPyL, a PSMA-based PET imaging agent for prostate cancer. *Clin Cancer Res*. 2011;17(24):7645–7653.
64. Ulmert D, Evans MJ, Holland JP, et al. Imaging androgen receptor signaling with a radiotracer targeting free prostate-specific antigen. *Cancer Discov*. 2012;2(4):320–327.
65. Wieser G, Mansi R, Grosu AL, et al. Positron emission tomography (PET) imaging of prostate cancer with a gastrin releasing peptide receptor antagonist – from mice to men. *Theranostics*. 2014;4(4):412–419.
66. Markwalder R, Reubi JC. Gastrin-releasing peptide receptors in the human prostate: relation to neoplastic transformation. *Cancer Res*. 1999;59(5):1152–1159.
67. Counsell RE, Schwendner SW, Meyer KL, Haradahira T, Gross MD. Tumor visualization with a radioiodinated phospholipid ether. *J Nucl Med*. 1990;31(3):332–336.
68. Pinchuk AN, Rampy MA, Longino MA, et al. Synthesis and structure-activity relationship effects on the tumor avidity of radioiodinated phospholipid ether analogues. *J Med Chem*. 2006;49(7):2155–2165.
69. Ibrahim N, Hall L, Fourzali Y, et al. Relative biodistribution and tumor uptake of 124I-CLR1404 (aka NM404) in non-small cell lung cancer (NSCLC) patients. *J Nucl Med*. 2013;54 Suppl 2:278.
70. Pickhardt PJ, Hall LT, Lee M, et al. A novel "diapeutic" molecular imaging agent for combined oncologic diagnosis and therapy in a broad spectrum of human cancers: preliminary clinical experience with CLR1404. *J Clin Oncol*. 2014;32 Suppl 5s:11000.
71. Rajagopalan KN, DeBerardinis RJ. Role of glutamine in cancer: therapeutic and imaging implications. *J Nucl Med*. 2011;52(7):1005–1008.
72. Smolarz K, Krause BJ, Graner FP, et al. (S)-4-(3-18F-fluoropropyl)-L-glutamic acid: an 18F-labeled tumor-specific probe for PET/CT imaging – dosimetry. *J Nucl Med*. 2013;54(6):861–866.
73. Qu W, Oya S, Lieberman BP, et al. Preparation and characterization of l-[5-11C]-glutamine for metabolic imaging of tumors. *J Nucl Med*. 2012;53(1):98–105.